WELDING RESEARCH

SUPPLEMENT TO THE *WELDING JOURNAL*, FEBRUARY 1990

Sponsored by the American Welding Society and the Welding Research Council

All papers published in the *Welding Journal's* Welding Research Supplement undergo Peer Review before publication for: 1) originality of the contribution; 2) technical value to the welding community; 3) prior publication of the material being reviewed; 4) proper credit to others working in the same area; and 5) justification of the conclusions, based on the work performed.

The names of the more than 170 individuals serving on the AWS Peer Review Panel are published periodically. All are experts in specific technical areas, and all are volunteers in the program.

Electrode Geometry in Resistance Spot Welding

Mathematical model predicts current distribution as a function of electrode geometry

BY R. J. BOWERS, C. D. SORENSEN AND T. W. EAGAR

ABSTRACT. The effect of electrode geometry on current distribution has been investigated. A mathematical model was developed to evaluate current distribution in both truncated cone (TC) and pimple-tipped (PT) electrodes. Electrode life and lobe curve tests were conducted to substantiate the results of the modeling effort. Results of the computational investigation showed that electrode sheet interface angles approaching 90 deg provide more uniform current distribution at the electrode face. Electrode geometry was shown to affect wear and life by its influence on local current distribution. Also, electrode geometry shifted the position of the welding lobe. It was concluded that efficient electrode design must balance mechanical and thermal properties as well as maintain current uniformity.

Introduction

With an average automobile containing approximately 5000 spot welds, the automotive industry is a major user of resistive welding technology. Of particular importance to the industry is the resistance welding of various galvanized sheet steel products, which have become established for use in automotive manufacture due to their corrosion resistance. However, this increased corrosion protection is offset by the increased difficulty of welding galvanized as opposed to uncoated steel. Alloying of the zinc coating with the copper electrodes used in spot welding promotes rapid wear, subsequently reducing electrode life.

Improving the weldability of galvanized steel has been approached by many methods, mainly those concerning the physical properties of the steel, such as coating composition, type and surface condition. The roles of welding parameters such as upslope, preheat and weld time also have been analyzed to determine their effects on weldability. Aspects of the electrode itself, such as material (Ref. 1) and geometry (Ref. 2), have been studied as well.

Friedman and McCauley (Ref. 3) concluded in their study that an uneven heating condition across the electrodes was one factor that contributed to an increased rate of electrode tip deformation. They explained this uneven heating in terms of variations in surface resistance due to nonuniformities in the steel coating. The present study approached the weldability of galvanized steel in terms of this uneven heating at the electrode face. However, unlike Friedman and McCauley, electrode geometry and its effect on current uniformity were considered as a source of uneven heating across the electrode face. Nonuniform current in this region would give rise to uneven heating, which could promote localized wear.

Kaiser, *et al.* (Ref. 4), in a study of weld nugget formation, noted an annular molten zone around the periphery of some welds. This phenomenon was noted by Lane, *et al.* (Ref. 5), who hypothesized that current distribution and electrode geometry significantly affect heat generation in the molten zone. Holm (Ref. 6) explained that a current constriction occurs at the

KEY WORDS

Resistance Welding
Spot Welding
Electrode Geometry
Current Distribution
Mathematical Model
Lobe Curve
Welding Lobe
Electrode Design
Electrode Life Tests
Galvanized Steel

R. J. BOWERS, C. D. SORENSEN and T. W. Eagar are with the Materials Processing Center, Massachusetts Institute of Technology, Cambridge, Mass.

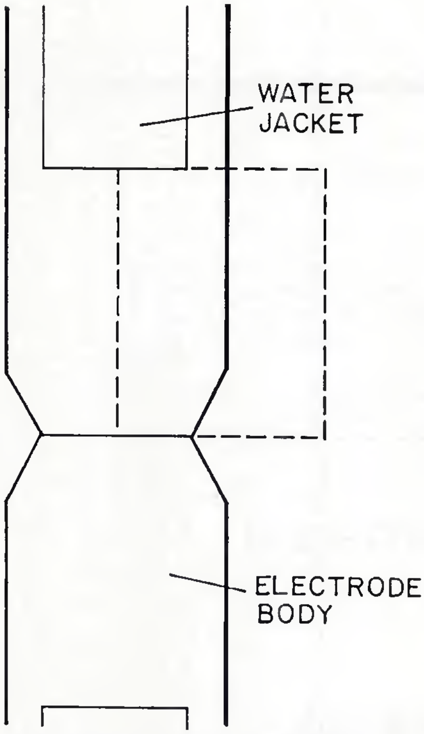

Fig. 1 — Modeled electrode configuration. Due to symmetry, only the boxed region is required to be modeled.

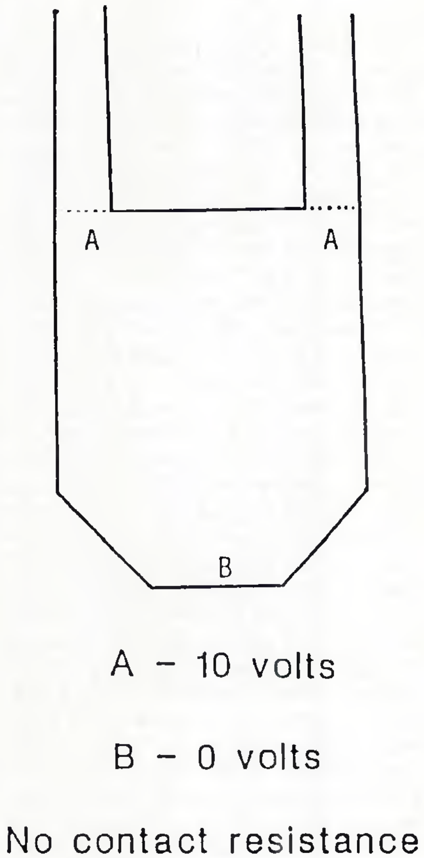

Fig. 3 — Model boundary conditions.

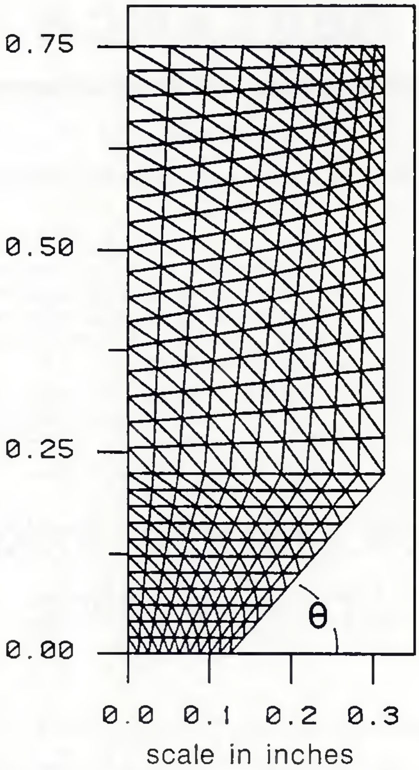

Fig. 2 — Finite element grid of TC electrode. Cone angle is marked as theta.

electrode face, with a disproportionate amount of current flowing through the outer face edge. Such a phenomenon would aid in explaining the observation of an annular molten zone at the periphery of a spot weld.

Numerical modeling of the spot welding process has also shown a current constriction at the electrode face edge. Greenwood (Ref. 7) noted that the current in resistance welding does not flow directly across the material being welded, but diverges into the worksheet. Furthermore, he stated that most of the current that spreads into the sheet enters near the electrode edge, causing a current constriction at that location.

Greenwood further stated that the initial temperature patterns show a maximum in a ring around the edge of the electrode. He concluded that if the current is high enough to produce a weld in such a short time, a ring weld will result. Such ring welds have been noted in the automotive industry. The results of Nied (Ref. 8) concur with those of Greenwood, showing both a current concentration at the periphery of contact between the electrode and the workpiece, as well as an initial temperature maximum in this area.

The existence of a current concentration at the outer edge of the electrode face is in agreement with the fact that current constricts around corners. Such a corner is found in the angle between the tapered end of a truncated cone electrode and the worksheet. However, the effect of this angle on the degree of current constriction has not been studied previously. This study used mathematical modeling to quantify effect of electrode geometry on current distribution at the electrode face and tested the results to determine a relationship between electrode geometry and electrode life.

Mathematical Modeling

Mathematical modeling, based on a finite element analysis (FEA) program developed by Segerlind (Ref. 9), was used to map the potential distribution along two electrodes in face contact. Only one quadrant of this configuration was required for modeling due to the ability of the model to accommodate axisymmetric geometries and due to the added symmetry of the configuration about the electrode faces — Fig. 1.

The geometry was discretized by the model into an array of connected elements — Fig. 2. Subject to the boundary conditions imposed on the geometry and the physical equations describing its interior, a response for each element was calculated so as to maintain continuity between all the elements.

The Laplace equation, $\nabla^2\phi = 0$, where ϕ is the electrical potential, was used to describe the electrode interior. This is correct for a DC current or when the magnetic skin depth of the electrodes is large with respect to the electrode radius. This latter condition is valid for copper alloy electrodes.

As it was not the intent of this investigation to produce an exhaustive mathematical model describing the resistance welding process, electrical conductivity was considered constant for the purposes of this model. Localized current concentrations give rise to localized resistive heating, which lowers electrical conductivity and tends to concentrate current elsewhere. This effect could be countered by decreased surface asperity at the outer edge of the electrode face, due to the friction hill effect, or molten zinc at the periphery of the weld due to the large initial current densities, giving rise to an easy current flow path. Since such effects occur in all electrode geometries, the assumption of temperature-independent electrical conductivity was judged to be valid in comparing current uniformity among different electrode geometries.

The model boundary condition consists of a 10-V potential drop across the electrode body — Fig. 3. This is not an actual welding condition; however, it was chosen to allow ease of scaling and comparison of results from different electrode geometries. A 10-V isopotential was positioned along the outer 0.10 in. (0.25 cm) of the electrode radius in the plane where the water jacket meets the electrode body. This condition is based on the assumption that the current density in the wall surrounding the water jacket is uniform and axial. A zero-volt isopotential was positioned along the intersection of the electrode faces. The high contact resistance occurring at the electrode-sheet interface, as compared to the resistance within the copper electrode, ensures an isopotential at this interface.

FEA was utilized to map the voltage potential within the electrode. The finite element mesh was finer near the electrode face to obtain a more accurate solution in this, the region of primary interest. Upon obtaining the voltage map, postprocessing determined the location of isopotentials within the electrode geometry. The model computed voltage values at the corners or nodes of the triangular elements within the geometry; the potential values within the elements were determined by linear interpolation.

Current density at the electrode face was calculated as the product of electrical conductivity and the gradient of the potential at the electrode face. The potential gradient at the electrode face was determined from voltages at small displacements from points along the face, using the formula:

$$\bar{J} = \sigma \nabla \phi$$

where $\bar{J}$ is the current density and σ is the electrical conductivity.

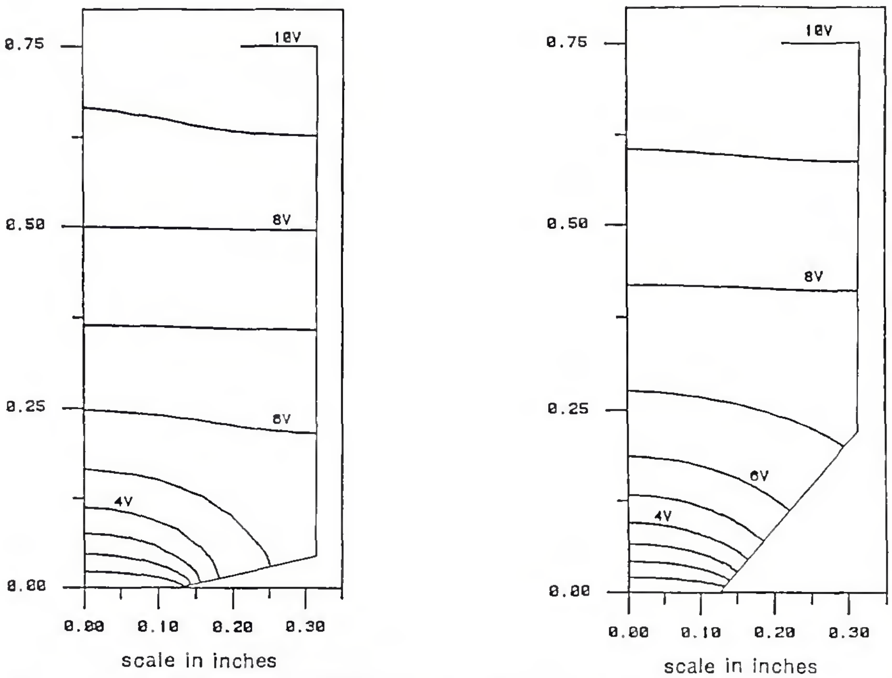

Fig. 4 — Isopotential maps of 15- and 50-deg truncated cone electrodes.

Truncated Cone Results

Isopotential maps were computed for two different truncated cone (TC) electrodes with cone angles of 15 and 50 deg — Fig. 4. For these geometries, the isopotentials near the electrode face exhibited a basic similarity; they were more widely spaced at the face center than at the face edge. Since current density is inversely proportional to isopotential spacing, a higher current density was present at the face edge than at the face center for the TC electrodes.

Current density profiles for the 15- and 50-deg TC electrodes were computed and scaled for a common total current of 10,000 A — Fig. 5. The degree of current nonuniformity present in the profiles was quantified by computing the ratio of the current density at the outside edge of the electrode face to the current density at the center of the electrode face. This ratio was computed to be 4.6 for the 15-deg TC electrode and 1.9 for the 50-deg electrode. Figure 6 shows the current density ratio for several different TC geometries.

Gould (Ref. 10) suggested that the face diameter influences electrode life. Further modeling was undertaken to determine if other aspects of TC electrode geometry affected the current density ratio. Results indicated that the ratio is fixed for a given cone angle. Changing the face diameter or the outside electrode diameter had no effect on the ratio; hence, the principles described herein cannot be used to explain Gould's results.

Current nonuniformity, as measured by the current density ratio, was found to decrease with increasing TC angle. The model confirmed that a uniform current distribution (ratio equal to 1.0) exists for a 90-deg cone angle. This geometry is simply a right circular cylinder.

Pimple-Tipped Results

Modeling results showed a trend for isopotentials to become flat, indicative of a uniform current distribution, in regions where the geometry of the electrode is straight and of constant radius. Pimple-tipped (PT) electrodes, the tips of which exhibit these characteristics as well as having a 90-deg contact angle, were modeled to determine the effect of tip diameter and tip length on current uniformity at the electrode face — Fig. 7.

Sixteen different PT geometries were modeled. Tip diameters ranged from 0.063 to 0.250 in. (0.160 to 0.635 cm). Each geometry was characterized by an aspect parameter, the ratio of the tip diameter to the tip length, D/L. This parameter ranged from 0.5 to 5.0.

It was expected that the PT geometry

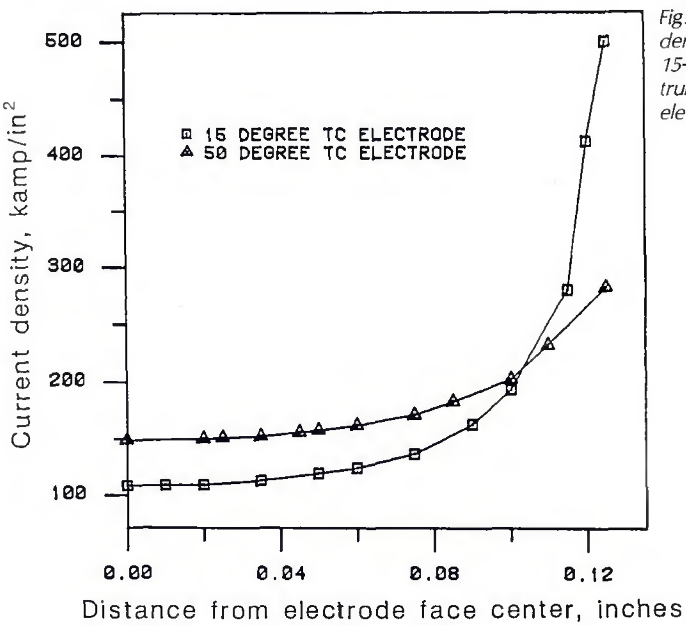

Fig. 5 — Current density profiles for 15- and 50-deg truncated cone electrodes.

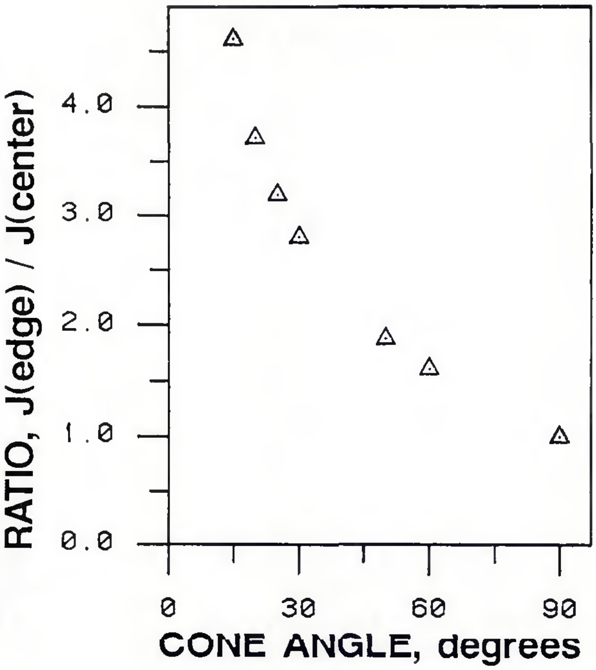

Fig. 6 — Current density ratio increases with decreasing cone angle for truncated cone electrodes.

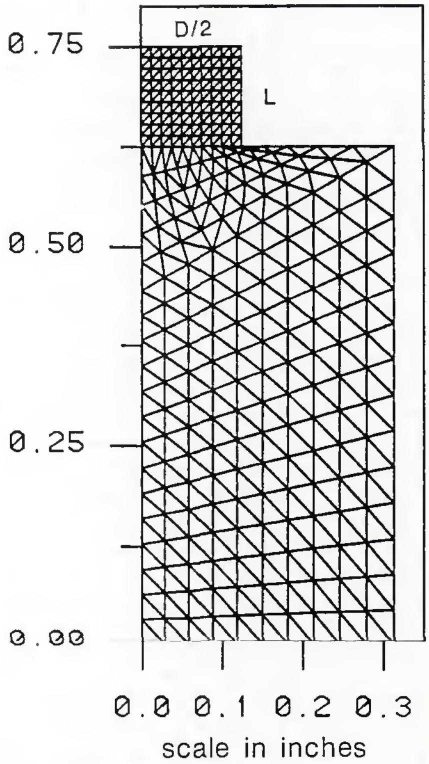

Fig. 7 — Finite element grid of PT electrode. Tip aspect ratio is D/L.

would exhibit greater current uniformity than the TC geometry due to its 90-deg contact angle. Modeling results confirmed this prediction. For the aspect parameters modeled, current density ratio ranged from 1.0 to 1.3, indicative of uniform current distribution — Fig. 8. The lowest ratios were observed for electrodes with lower aspect parameters having long thin tips.

Modeling Discussion

In terms of current density uniformity, the PT geometry was shown to be superior to the TC geometry. The PT geometry exhibited a nearly uniform current distribution at the electrode face, whereas the TC geometry exhibited large current concentrations at the outer electrode face edge.

It was reasoned that geometries exhibiting large current densities near the outer face edge would exhibit different welding characteristics than geometries with more uniform current distributions. Since during the resistance welding process current diverges into the worksheet, the presence of a large current concentration near the outer edge of the electrode face would leave less current available for nugget formation at the faying interface directly beneath the electrodes.

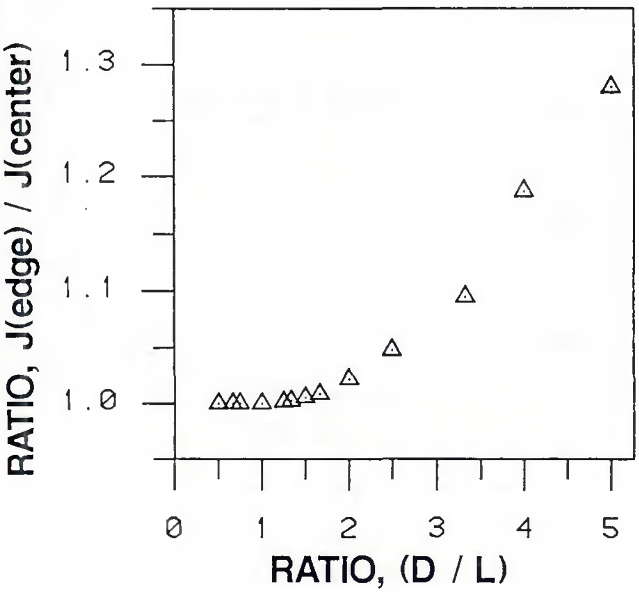

Fig. 8 — Current density ratio increases with increasing aspect parameter for PT electrodes.

It was predicted that geometries with large current density ratios would require greater RMS current values to achieve both nominal weld nugget size and expulsion. Thus, the lobe curve of a material welded with such electrodes would be shifted to higher current values. Increased current nonuniformity was also predicted to adversely affect electrode life due to greater localized wear.

Experimental Procedure

Lobe curve determinations and electrode life tests were conducted using a 75 kVA pneumatic press spot welding machine equipped with a synchronous controller. Force readings were determined by the pressure differential between two air gauges. RMS current values were determined by a toroidal coil current meter. TC electrodes were used for testing because of the wide range in current uniformity achievable with different cone angles, and the ease of machining these geometries. All electrodes were RWMA Class II copper-chromium alloys.

Lobe curve values were the average of at least two tests. Three tests were conducted for a given time-current combination if the difference between the initial values exceeded 350 A (RMS). For this investigation, the maximum electrode life was established when the weld nugget size dropped below the specified nominal nugget size for more than 100 welds. Life tests were conducted at currents just be-

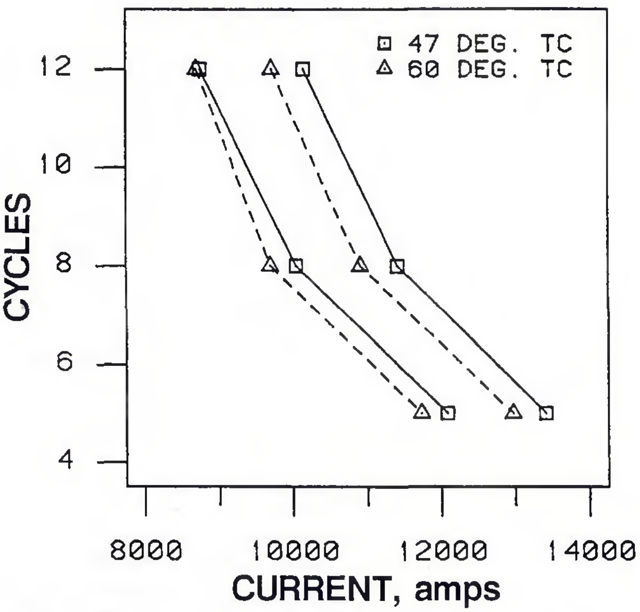

Fig. 9 — Lobe curves for 0.031-in. G60 hot-dip galvanized sheet steel. Analysis revealed the observed lobe shift is not statistically significant.

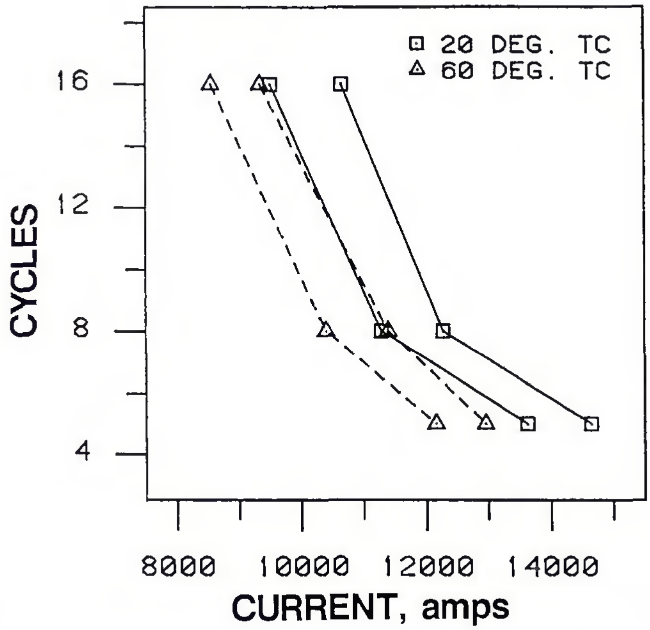

Fig. 10 — Lobe curves for 0.031-in. electrogalvanized sheet steel with coating weight 68 g/m². The approximately 1000-A lobe shift is statistically significant.

low the expulsion limit of the particular galvanized steel being welded.

For both lobe and life tests, the electrodes were conditioned for 50 welds prior to testing. Average nugget size was determined by at least two peel tests. In the case of elliptically shaped nuggets, the geometric mean of the large and small diameters was calculated as an effective diameter.

Lobe Curve Results

In the first series of lobe curve tests, 47- and 60-deg TC electrodes were used to weld Steel A — Table 1. The lobe curves for this steel revealed a shift to lower RMS current values for the 60-deg electrode — Fig. 9. This result was expected since the 60-deg electrode was shown to exhibit a more uniform current distribution at the electrode face. However, statistical analysis of the lobe curve data revealed that, despite the observed shift, the two data sets could not be statistically separated at the 90% confidence level.

A second set of lobe curves were determined using 20- and 60-deg TC electrodes to weld Steel B. The difference between the cone angles was increased from the first test to increase the range of current nonuniformity. The results exhibited a large shift to lower RMS current values for the 60-deg TC electrode — Fig. 10. Analysis of these data sets at the 90% confidence level revealed the lobe shift to be statistically significant. For the six tested time-current combinations of the lobe curves, the average lobe shift was from 850 A at the low end of the confidence interval to 1550 A at the high end of the confidence interval.

Life Test Results

Two sets of electrode life tests were conducted; the first tests of each set were conducted with 15-deg TC electrodes, the second with 60-deg TC electrodes. Steels A and C (Table 1) were tested. For both sets of tests, the 15-deg electrode exhibited shorter life.

For Steel C, the 15-deg electrode life was 2400 welds, compared to 3200 welds for the 60-deg electrode — Fig. 11. For Steel A, the 15-deg electrode failed at 750 welds, whereas the 60-deg electrode produced nuggets well above nominal size at 900 welds — Fig. 12.

Discussion of Experimental Results

From the modeling effort, it was learned that electrode geometry affects current distribution, with higher electrode-to-worksheet angles exhibiting more uniform distributions. A correlation can be drawn between current distribution and lobe curve position by considering the experimental results.

The 60-deg TC electrode required ap-

Table 1—Steel Characterization

Steel	A	B	C
Sheet thickness	0.031 in.	0.031 in.	0.056 in.
Coating type and process	G60 hot dip	68 g/m² electro-galvanized	A40 galvannealed
Welding force[(a)]	650 lb	500 lb	1000 lb

(a) The welding force listed is the force that produced the widest lobe width for the materials with an 8-cycle weld.

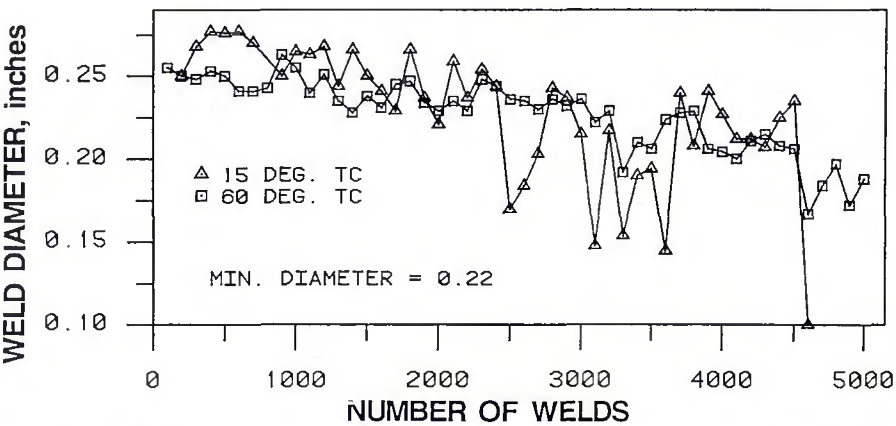

Fig. 11 — Life test results for 0.050-in. galvannealed steel. Minimum required weld nugget diameter is 0.22 in.

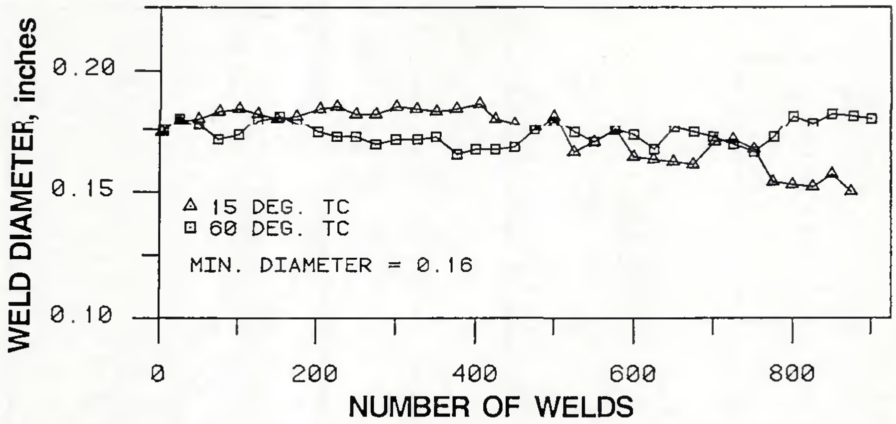

Fig. 12 — Life test results for 0.031 G60 hot-dip galvanized steel. Minimum required weld nugget diameter is 0.16 in.

proximately 1000 less amperes (RMS) to produce a weld of nominal size than the 20-deg TC electrode. Since the higher angle electrode has a more uniform current distribution, it was concluded that current uniformity at the electrode face shifts the lobe curve to lower current values.

By shifting the lobe curve, electrode geometry plays a dual role in electrode life. Low-angle electrodes exhibit large current concentrations at the electrode face edge. This effect is exacerbated by the fact that the electrode life test current (just below expulsion) was increased for low-angle TC electrodes due to the lobe shift. Increased total current and greater current nonuniformity help to explain why the low-angle TC electrode exhibited a shorter life in this investigation.

However, thermal and mechanical properties must also be considered in the electrode life equation. Lower angle TC electrodes, by providing a larger mass at the tip, exhibit greater thermal and mechanical benefits. Hence, in the absence of a nonuniform current distribution, low-angle geometries would be expected to exhibit longer tip life. Indeed, as spot repetition rates and welding pressure increase, thermomechanical stiffness may become a dominant factor affecting tip life.

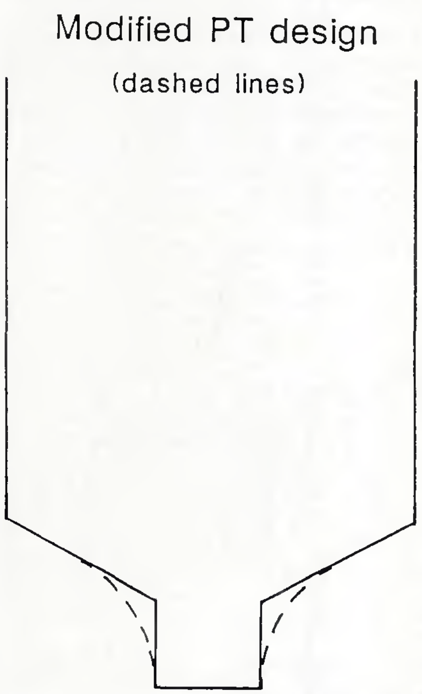

Fig. 13 — Proposed electrode design provides greater strength, a larger heat sink and a uniform current distribution.

Electrode Design

A relation between electrode geometry, current distribution and electrode life was formulated from the results of the modeling and experimental testing. Higher electrode-worksheet interface angles were shown to yield more uniform current distributions at the electrode face. This effect reduces localized heating at the face periphery. This more uniform heating may contribute to more even wear, even though higher angles promote more rapid mushrooming of the tips. Also, more uniform current distributions were shown to require lower RMS current values to produce nominal size welds.

However, a contact angle of 90 deg, as in PT electrodes, results in a tip that neither has the mechanical strength of a low-angle TC electrode nor provides a large heat sink, both of which are valuable at increased spot rates and higher welding pressures. Thus, good electrode design involves a trade-off between current uniformity and thermomechanical stiffness. Both the loss of current uniformity and the loss of mechanical stiffness promote wear; the geometry that promotes one, however, tends to minimize the other.

It is believed that an optimum electrode geometry exists that balances these two competing mechanisms of wear. One possible design consists of a contact angle of 90 deg at the electrode face edge to the outer electrode diameter — Fig. 13. This design would provide greater mechanical strength and a larger heat sink at the tip than the PT geometry, while maintaining a 90-deg contact angle, which provides the most uniform current. Also, the radius could be changed to favor either mechanical strength or current uniformity.

A test batch of electrodes with this design were machined for testing on galvanized material (Ref. 11). Preliminary results of those tests showed an increase in electrode life from 800 to 2000 welds over the electrode geometry that was in use. Also, the required welding current was shifted from 16,000 to 13,000 A. However, the design was reported to be less tolerant of misalignment as radiused-tip or TC electrodes due to its high electrode-worksheet interface angle.

Conclusions

It is important to note that the mathematical model developed herein is a first-level approach to understand the trends produced in current distribution as affected by electrode geometry. It is most interesting that the experimental results support the predictions derived from the model, despite the model not incorporating such factors as contact resistance, alloying and deformation of the electrode tips and the temperature dependence of electrical conductivity of the electrode material. Yet, the experimental results support the predictions derived from the modeling effort. The shifted lobe position and longer electrode life obtained merely by changing the electrode geometry indicate that geometry is a controlling process variable for a given set of welding parameters.

Investigation of the effect of electrode geometry on current distribution by both mathematical modeling and experimental testing led to several conclusions.

1) Electrode sheet interface angles approaching 90 deg provide more uniform current distributions at the electrode face.

2) Electrode geometry can affect wear and life through its influence on the local current distribution.

3) Electrode geometry shifts the position of the welding lobe.

4) Efficient electrode design must provide for thermal and mechanical stiffness as well as maintain current uniformity.

Acknowledgments

The authors wish to thank the General Motors Corp., the International Lead Zinc Research Organization and Ford Motor Corp. for funding this research. Also acknowledged are Dr. Min-Long Lin for his work with the computer modeling, and Christopher Walton and Andre McFayden for their aid in the experimental testing. Thanks also goes to Tom Natale of National Steel, who provided the galvanized sheet steels for the research.

References

1. Simmons, W. P. 1967. Spot welding electrode life. *Welding Journal* 46(11):915–920.
2. Nadkarni, A. V., and Weber, E. P. 1977. A new dimension in resistance welding electrode materials. *Welding Journal* 56(11):331-s to 338-s.
3. Friedman, L. M., and McCauley, R. C. 1969. Influence of metallurgical characteristics on resistance welding of galvanized steel. *Welding Journal* 48(10):454-s to 462-s.
4. Kaiser, J. G., Dunn, G. J., and Eagar, T. W. 1982. The effect of electrical resistance on nugget formation during spot welding. *Welding Journal* 62(6):164-s to 174-s.
5. Lane, C. T., Sorensen, C. D., Hunter, G. B., Gedeon, S. A., and Eagar, T. W. 1987. Cinematography of resistance spot welding of galvanized steel. *Welding Journal* 66(9):260-s.
6. Holm, R. 1967. *Electrical Contact: Theory and Application*, pp. 9–18, New York, Springer-Verlag.
7. Greenwood, J. S. 1961. Temperatures in spot welding. *British Welding Journal*, 8(6):316–322.
8. Nied, H. A. 1984. The finite element modeling of the resistance welding process. *Welding Journal* 63(4):123-s to 132-s.
9. Segerlind, L. 1976. *Applied Finite Element Analysis*. New York, John Wiley and Sons.
10. Gould, J. E., and Chang, P. H. 1986. The effect of welding time and electrode diameter on electrode life when resistance spot welding galvanized steel. *Proc. Sheet Metal Welding Conference II*. AWS Detroit Section, Detroit Mich.
11. Bush, A. W. Private communication. April 1987. CMW, Inc., Indianapolis, Ind.